Your Vision, Our Future

Important Characteristics of
Sound Fields of Ultrasonic Transducers

Important Characteristics of Sound Fields of Ultrasonic Transducers

By K. A. Fowler, F. H. C. Hotchkiss, T. V. Yamartino, and T. Nelligan

Author note: Original paper written Kenneth Fowler, Frederick Hotchkiss, and Tom Yamartino and published by Panametrics, Inc., in 1983. Web version edited and updated in 2012 by Tom Nelligan.

I. Definitions
II. Sound Fields of Flat Circular Disk Transducers
III. Focusing Effects
IV. Attenuation effects

I. Definitions

Throughout the literature concerned with ultrasonic transducers and their characteristics, a variety of notations and symbols has been used. What follows is an attempt to provide a useful set of definitions and a consistent set of notation. Where possible, notation has been selected that is used most frequently in technical literature.

Transducer: A device that is capable of converting one for of energy into another form. In the case of ultrasonic transducers, electrical energy is converted to mechanical (sound) energy and vice versa.

Transducer assembly: A mechanical assembly containing the transducer or transducers, that provides protection, damping, electrical matching, and connections, all in a package that is physically convenient to handle. Informally, ultrasonic transducer assemblies used in NDT are usually referred to simply as "transducers".

Velocity of sound: Refers to the speed at which sound waves travel through a transmissive material. The velocity of sound depends on the material and the mode of wave propagation. To a lesser extent the velocity of sound will depend on temperature, and the processing history of the material. Sound velocity is usually expressed in meters per second or incher per microsecond. The notation for sound velocity is c.

Mode of sound propagation: Sound waves can travel in solids in a variety of ways, usually called modes of propagation. The two most common modes are longitudinal and shear waves. Surface (Rayleigh) and plate (Lamb) wave modes are also important in some flaw detection techniques. Liquids and gasses transmit only longitudinal waves.

Frequency: The number of oscillations per second of the wave produced by a transducer. In ultrasonic testing, frequency is commonly used to describe the nominal or design center frequency of a transducer. Frequency is usually expressed in Megahertz (MHz) and the notation for frequency is f.

Wavelength: The distance a sound wave travels in one period (τ) in a given material. The notation for wavelength is λ .

$$\tau = 1/f \qquad (1)$$
$$\lambda = c\,\tau \qquad (2)$$
$$\lambda = c/f \qquad (3)$$

Bandwidth: The operating frequency range of a transducer assembly is its bandwidth. For pulse/echo transducers (see Figure 1), it is defined as the difference between the upper (f_u) and lower (f_l) frequencies at which the pulse/echo signal amplitude is 6 dB down from the frequency at which maximum signal amplitude occurs. Bandwidth is an important characteristic of ultrasonic transducer assembles. It is usually measured from the amplitude versus frequency spectrum using a spectrum analysis software. The apparent bandwidth and details of the spectral response of a transducer assembly are dramatically influenced by the electrical characteristics of the pulser/receiver, cable type and length, electrical matching, target shape, and the attenuation characteristics of the test material.

$$\text{Bandwidth} = f_u - f_l \qquad (4)$$

$$\text{Percent bandwidth} = \frac{f_u - f_l}{f_c} \; x \; 100\% \qquad (5)$$
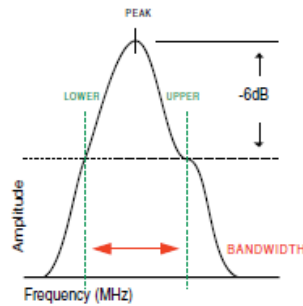
Figure 1 – Typical frequency response spectrum of pulse-echo transducer

Center frequency: Used in the above bandwidth calculation, is defined as

$$\text{Center frequency} = f_c = \frac{f_u + f_l}{2} \qquad (6)$$

Note that center frequency may not be the frequency at which maximum pulse/echo signal amplitude occurs.

Peak Frequency: Is defined as the frequency at which maximum pulse/echo signal amplitude occurs. Its notation is f_p. See Figure 1.

Decibel (dB): The unit used to express the ratio of one amplitude or power level relative to another. In ultrasonic NDT, this is usually the ratio of echo amplitudes.

For signal amplitudes measured in volts:

$$dB = 20 \log_{10} (V_1 / V_2) \qquad\qquad (7)$$

For power measured in watts:

$$dB = 10 \log_{10} (W_1 / W_2) \qquad\qquad (8)$$

Near Field (Fresnel Zone) : The part of the sound field between the transmitting surface of the transducer assembly and the point on the acoustic axis where the past pulse/echo maximum occurs is called the near field. The point at which the last pulse/echo maximum occurs is sometimes designated as the Y_0+ point. We will define this distance as N. The following relationships hold exactly only for long pulse or continuous wave excitation. Note also that the equations are for single frequency sources, while ultrasonic transducers used in NDT typically generate energy across a spectrum of frequencies.
(a) For a circular disk transducer:

$$N = r^2/\lambda \ - \ \lambda/4 \qquad \text{where r = radius of the disk} \qquad (9)$$

Most texts simply use $N = r^2/\lambda$ and ignore the $\lambda/4$ term. For most cases, where transducer radius is large with respect to wavelength, this is satisfactory. However, as Rose [1] points out, results can be misleading for small diameter, low frequency transducers operating into high velocity materials such as steel.

Equation 9 can be rewritten as

$$N = \frac{r^2}{\lambda}\left[1-\left(\frac{\lambda}{D}\right)^2\right] \qquad \text{where D is the diameter of the element.} \qquad (10)$$

The percent error in N calculated from r^2/λ is then $(\lambda/D)^2$ x 100%. Therefore, a $D/\lambda = 10$ produces a 1% error in N while a $D/\lambda = 5$ gives an error of 4% and for $D/\lambda = 2$ the error is 25%. In other words, for $D/\lambda = 2$, N is actually 25% shorter than the value calculated by r^2/λ .

(b) For a square transducer:

$$N = \frac{1.42 \, A^2}{4\lambda} \qquad \text{where A is the length of a side of the square} \qquad (11)$$

<u>Far Field (Fraunhofer Zone)</u>: The far field is the region beyond the near field where beam spreading occurs and the pulse/echo signal amplitude from small on-axis reflectors diminishes as $1/Z^2$ where Z is the distance from the radiating surface of the transducer assembly.

<u>Beam Spread Angle</u>: The angle of divergence of the main lobe of the sound field, as seen in Figure 2 below. The notation for the beam spread angle is α, and the angle is measured between the acoustic axis at a point in the far field and the point moving in the transverse direction where the acoustic pressure first reaches a specified minimum (commonly -6 dB from peak). It is the angle at which exact phase cancellation occurs in the far field at a single operating frequency. The beam spread angle in pulse/echo mode is commonly calculated as follows:
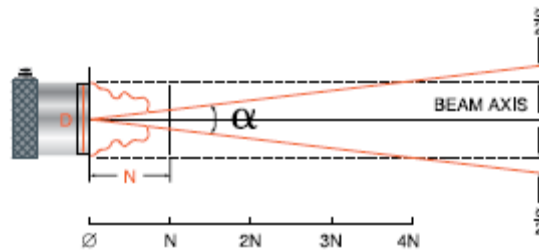
$$Sin\ (\alpha/2)\ =\ .514c\ /\ fD$$

where α/2 = half angle spread between -6 dB points
  c = sound velocity in the test medium
  f = frequency
  D = transducer diameter

Which can also be expressed as

$$Sin\ (\alpha/2)\ =\ .514\lambda\ /\ D$$

Figure 2 shows a generalized representation of this concept


Figure 2 – Beam Spread Angle

The -20 dB beam spread angle can be similarly calculated from the formula

$$Sin\ (\alpha/2)\ =\ .870c\ /\ fD$$

In the case of typical disk transducers, if sound pressure in the far field was measured with a small hydrophone in a 180 degree semicircle at a fixed distance from the transducer, a series of minima followed by maxima of decreasing amplitude would be observed. Figure 3 shows two representations of a typical result, in linear and polar plots.
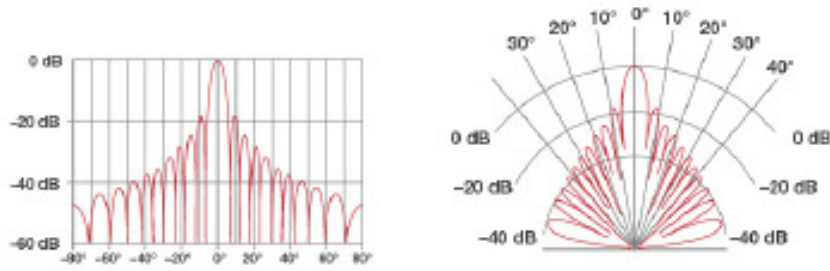
Hydrophone output versus angle   Polar plot of graph at left

Figure 3 – Two representations of lobe structure of single frequency sound field produced by a circular disk transducer

For circular disk transducers, the angular positions of the minima are given by

$$\text{Sin } \theta_n = (1.22 + n - 1)(\lambda / D) \quad n = 1, 2, 3 \ldots \qquad (13)$$

For a square transducer, the angular positions of the minima are given by

$$\text{Sin } \theta_n = n\lambda / A \text{ where A = side dimension of the square} \qquad (14)$$

Note that in ultrasonic testing, transducers are most commonly excited by short pulses containing a spectrum of frequencies rather than a single frequency. Depending on the bandwidth of the radiated pulse, the lobe structure of the sound field will be more or less obliterated. For broadband pulses, the values of n can be used to determine the angles at which the sound pressure as measured with a hydrophone has dropped by approximately 10 dB, 20 dB, 25 dB, and 30 dB for n = 1, 2, 3, and 4 respectively.[3] In pulse/echo, this would suggest a 20 dB decrease in amplitude at the first minimum.

II. Sound Fields of Flat Circular Disk Transducers

A. Single Frequency Operation

The sound field produced by a flat circular transducer driven at a single frequency has been discussed by several authors.[3, 4, 5, 6] In most cases approximations have been used to simplify the analysis. A rigorous treatment of the baffled piston reflector containing no approximations is provided by Goodman.[8] The pressure field is then:

$$P\left(\vec{r}\right) = i f u_0 \rho \iint_S \frac{e^{-ikr'}}{r'} \left(1 - \frac{i}{kr'}\right) \cos \theta dS \qquad (15)$$

where u_0 = the maximum velocity at the radiating surface

ρ = the density of the transmitting material

k = $2\pi / \lambda$

$\vec{r}$ = position vector of the sound field point

r' = magnitude of the vector from the radiating surface to the field point

f = frequency

θ = angle between the sound field axis and the vector from the radiating surface to the sound field point

dS = the surface integral

i = $\sqrt{-1}$

At sound field distances significantly greater than one wavelength and for field points not too far off the center axis, equation 15 reduces to the usual Rayleigh integral:

$$P\left(\vec{r}\right) = i f u_0 \rho \iint\limits_S \frac{e^{-ikr'}}{r'} \, dS \qquad (16)$$

For on-axis calculations, the Rayleigh integral can be solved analytically; the complex expression (equation 15) can also be solved analytically on the axis, but off-axis points require numerical integration. For on-axis, the complete expression for sound pressure is:

$$P(z) = \rho u_0 cz \left(\frac{e^{-ikz}}{z} \right) - \frac{e^{-ik\sqrt{z^2 + a^2}}}{\sqrt{z^2 + a^2}} \qquad (17)$$

where c = the velocity of sound in the material

a = the radius of the transducer element

z = the distance between the transducer and the on-axis point

The on-axis pulse/echo response with CW or long pulse excitation is:

$$I(z) = (= \rho u_0 c)^2 \left(1 + \frac{z^2}{z^2 + a^2} - \frac{2z}{\sqrt{z^2 + a^2}} \cos\left[k\left(\sqrt{z^2 + a^2} - z \right) \right] \right) \qquad (18)$$

Equation 15 gives the proper behavior for the pressure field at all locations; at large distances it reproduces the well-verified results of the Rayleigh integral. At closer distances it gives the proper flattening of the transverse profile, and extremely close to the transducer face it approaches both numerically and in the mathematical limit a pressure equal to ($\rho u_0 c$), as the boundary conditions say it should.

When evaluated with the Rayleigh integral, the on-axis pressure oscillates with constant amplitude. The locations of the maxima are given by Posakony[9] as:

$$Z_{max(n)} = \frac{4a^2 - \lambda^2 (2N+1)^2}{4\lambda (2n+1)} \qquad n = 0, 1, 2 \ldots \qquad (19)$$

$$Z_{min(n)} = \frac{a^2 - \lambda^2 n^2}{2n\lambda} \qquad n = 1, 2, 3 \ldots \qquad (20)$$

Equations 19 and 20 can be combined to give the exact locations of the on-axis maxima and minima as:

$$Z_{max = n \text{ odd}, min = n \text{ even}} = \frac{a^2/\lambda}{n}\left[1 - \left(\frac{\lambda}{D}\right)^2 n^2\right] \qquad n = 1, 2, 3 \ldots \qquad (21)$$

where n cannot exceed a value that would produce a negative result.

Equation 18 has been evaluated for the points of Z_{max} and Z_{min} that given by equation 21 for two values of D/λ, $D/\lambda = 10$ and $D/\lambda = 50$. The results are shown graphically in Figure 4a. Note however that for $D/\lambda = 10$ the characteristic maxima and minima are moved towards the transducer when plotted against the Seki parameter $S = Z/N$ and, contrary to most published literature, the magnitude of the maxima diminishes with each maximum as the transducer is approached. This effect still prevails even at $D/\lambda = 50$ for smaller fractional values of near field length N. An isometric view of the pulse/echo transverse beam profile for $D/\lambda = 10$ calculated from equation 15 is shown in Figure 4b.
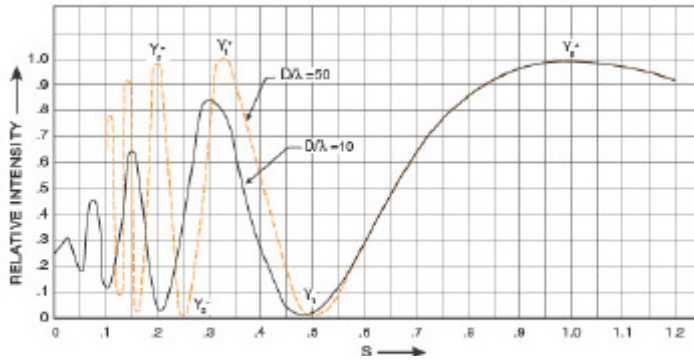
Figure 4a – Normalized axial pulse/echo response for circular disk transducer, $D/\lambda = 10$ and $D/\lambda = 50$
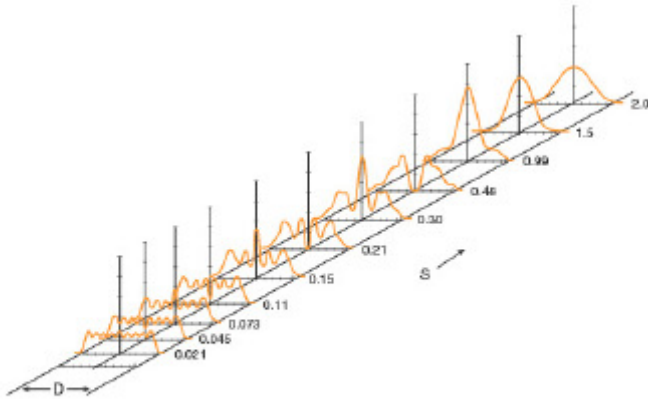
Figure 4b – Isometric view of normalized transverse pulse/echo response versus axial position for a circular disk transducer with D/λ = 10

The sound field is generally described as being divided into zones, the near field or Fresnel zone where interference effects occur, and the far field or Fraunhoffer zone where interference effects are absent. For n = 1, equation 21 reduces to

$$Z_{max} = N = a^2/\lambda - \lambda/4$$

This is the point at which the last on-axis pulse/echo maximum occurs.

The pulse/echo response in the near field of transducers with D/λ >> 10 is characterized by a series of on-axis maxima and minima. From equation 21 for D/λ >> 10, points of on-axis maxima occur at N and at the odd fractional distances of N/3, N/5, N/7, etc. The on-axis pulse/echo response is minimized at even fractional distances of N/2, N/4, etc. McMaster[6] is frequently quoted and uses a Y notation for these sound field landmarks as follows:

$$N = r^2/\lambda \quad \text{------} \quad Y_0^+ \quad (\text{"Y plus zero"})$$

$$N/2 \quad \text{----------------} \quad Y_1^-$$

$$N/3 \quad \text{----------------} \quad Y_1^+$$

$$N/4 \quad \text{----------------} \quad Y_2^-$$

$$N/5 \quad \text{---------------} \quad Y_2^+ \quad \text{etc.}$$

Because the transverse and axial pressure profiles vary greatly in the near field zone, quantitative flaw detection in this region is difficult with narrowband transducers. Many experts advise against using this portion of the sound field for flaw detection, although time domain tests such as thickness gaging or velocity measurement are generally unaffected.

In the far field, the on-axis sound pressure drops to zero with increasing distance, with pressure decreasing as 1/Z. For long pulsed CW excitation, the pulse/echo signal amplitude from a small on-axis reflector is proportional to intensity and drops to zero inversely with the square of distance, $1/Z^2$. The sound pressure also drops approximately in a Gaussian fashion in the transverse direction. However side lobes may be present, causing pressure maxima in the transverse direction, although these maxima will be lower in amplitude than the main lobe. The number and angular position of the side lobes, if present, are determined by transducer bandwidth and also by the ratio D/λ as described above.

Sound field characteristics can be measured experimentally using either pulse/echo measurements from a small ball reflector or by using a small hydrophone. The ball diameter should be less than or equal to ten wavelengths in order to approximate a point reflector. A hydrophone should be less than or equal to one-half wavelength in diameter. Either method can be used to survey sound fields, however the pulse/echo procedure is much more commonly used for evaluating transducers designed for nondestructive testing applications. The relative changes in signal amplitude measured by a hydrophone used to survey the transmitted sound field will be twice as large on a dB scale as the pulse/echo signal received from a ball target surveying the reflected sound field. In other words, a 0.707 fractional amplitude change (3 dB) measured with a small hydrophone is the equivalent of a 0.5 fractional change (6 dB) in a pulse/echo response at the same point in the sound field.

The preceding discussion has been limited to the characteristics of the sound fields produced by circular disk transducers operating at a single frequency, i.e. with continuous wave excitation. Transducer assemblies used for ultrasonic flaw detection and thickness gaging are typically designed to produce short direction pulses, which are necessary in order to achieve good near surface resolution. However, by definition, a short duration pulse contains a band of frequencies around the center frequency. The bandwidth of transducers commonly used for NDT applications ranges from about 20% to greater than 100%. Although the transducer bandwidth as well as other factors can modify the sound fields produced by single frequency operation, it is useful to understand the features of the single frequency sound field as a frame of reference.

B. Effects of Bandwidth

When a broadband transducer assembly is pulsed with a short duration electrical impulse, a band of frequencies is produced, and the resulting waveform is short in duration. At each coordinate point in the sound field of the transducer, the amplitude can be quantified by any of four measures: the peak positive half-cycle amplitude, the peak negative half-cycle amplitude, peak-to peak amplitude, or the peak rectified amplitude. This must be specified when discussing the pressure field or more appropriately the response map of a pulsed transducer.

To calculate the pressure field of a pulsed transducer, one must include all of the frequency components, each weighted according to the transducer's spectrum. The time

varied pressure detected by a point hydrophone and in pulse/echo reflection of a point reflector are given by:

$$P_{\text{hydrophone}}(r, t) = \int_{-\infty}^{\infty} \beta(\omega)\, P_0(r, \omega)\, e^{i\omega t}\, d\omega \tag{22}$$

$$P_{\text{pulse/echo}}(r, t) = \int_{-\infty}^{\infty} [\beta(\omega)\, P_0(r, \omega)]^2\, e^{i\omega t}\, d\omega \tag{23}$$

where $\beta(\omega)$ is the impulse response pulse spectrum (single transduction), $P_0(r, \omega)$ is the CW pressure contribution at the field point, and the rest of the expression represents the inverse Fourier transform from frequency domain to time domain.

An important feature of equations 22 and 23 is that the pulse/echo response map cannot be calculated by merely squaring the hydrophone response map. This is distinctly different from the CW case where the pulse/echo response is identical to the sound intensity distribution (the CW pressure squared).

Most flaw detector users customarily work with the peak of a full-wave rectified waveform. Figure 5a shows the on-axis pulse/echo bandwidth of a transducer with $D/\lambda_0 = 10$ and pulse/echo bandwidths of 20%, 40%, 60%, and 80%.
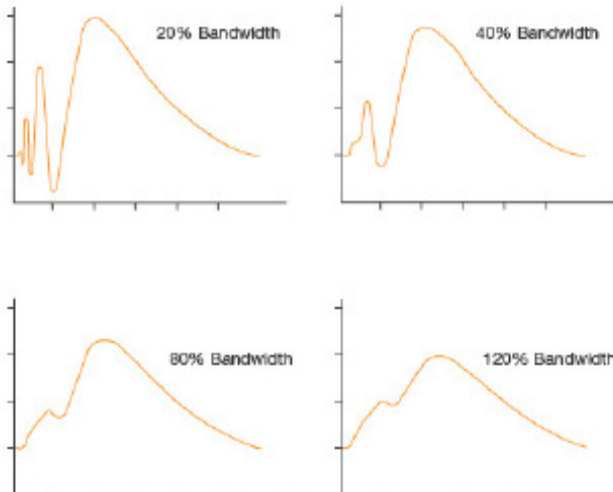
Figure 5a – Normalized axial pulse/echo response using full wave rectified peak for a circular disk transducer with $D/\lambda = 10$ and different bandwidths
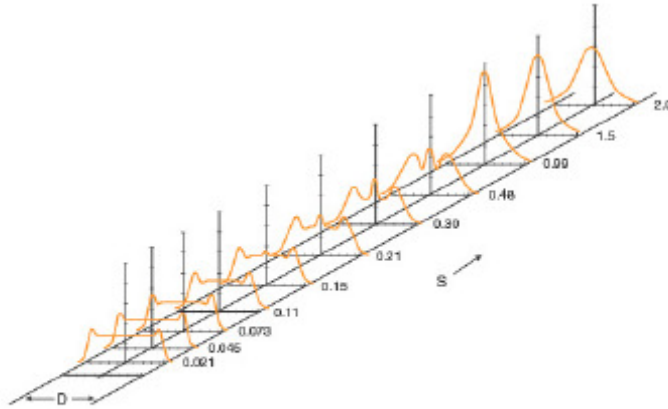
Figure 5b – Isometric view of normalized transverse pulse/echo response versus axial position using full wave rectified peak for a circular disk transducer with D/λ = 10 and BW = 80%

Note the comparison between Figure 5b and Figure 4a (the CW axial pulse/echo profile). The location of the last maximum also shifts from $N = r^2/\lambda_0$ at 20% bandwidth to about 1.2 N at 120% bandwidth. Figure 5b shows pulse/echo bandwidth of a transducer with $D/\lambda_0 = 10$ and 80% bandwidth using full-wave rectified peak detection. A comparison with the similar presentation of a single-frequency pulse/echo profile (Figure 4b) shows several differences. The most striking difference occurs in the near field, where the pulse/echo response is much more uniform. Although near field response differences tend to decrease with increasing bandwidth, there is minimal improvement at bandwidths above 80%. The origin of the smoothing is the combined effect of many frequency components, hence wavelengths, in the transmitted pulse. The exact value of the pulse/echo response at a given point in the sound field will depend not only on bandwidth, but also on the shape of the spectrum, and hence the energy level associated with each frequency component. However the effect of the broadband transmitted pulse is to smear characteristic features of the single frequency response map, so that there are no longer any nulls present.

From this it can be easily recognized that transducer as well as instrument bandwidth can have a significant effect on attempts to estimate the size of small flaws within the near field from signal amplitude and distance or depth.

III. Focusing Effects

Focused transducers represent an important class of transducer assemblies. They concentrate sound energy into a spot whose diameter is smaller than that of the unfocused beam from a transducer element of the same frequency and diameter, and their importance lies in the dramatically increased echo amplitudes that can be achieved when search for small defects within the focal zone and better definition of the beam for characterizing or sizing large flaws. They also offer better sound coupling into sharply curved test pieces like small diameter tubing and bars. Focused transducers are widely

used in immersion testing for improving the detectability of small flaws as well as for curved surface coupling. Focused transducers are also available for angle beam and delay line contact testing. This section is devoted to defining the focal characteristics of transducer assemblies in pulse/echo testing and the relationships controlling them. The theory is based on single frequency or long pulse operation. Modifications introduced by bandwidth are mentioned in the text. Figure 6 illustrates the geometry of a typical focused transducer using a refracting lens and a curved radiating surface.
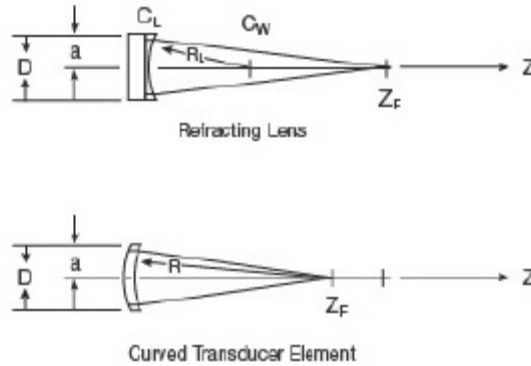
Figure 6 – Notation of parameters of focused transducer assemblies

Focal Length: The focal length of a transducer assembly is defined as the distance from the radiating surface to the point on the acoustic axis where maximum pulse/echo response from a point reflector like a small ball target occurs. The focal length of pulse/echo transducers is normally measured as the axial distance (Z) between the radiating surface and a defined reflector or target at which the amplitude of reflection signal is maximum. The focal length measured in this way will be significantly influenced by the reflector geometry, typically a small ball target versus a flat plate. The term for focal length is Z_F.

Normalised Focusing Length or Focusing Factor: In discussing the focusing characteristics of ultrasonic transducer it is often helpful to express the focal length as a percentage of the near field length. The normalized focal length S_F, sometimes called the focusing factor, is the actual focal length Z_F divided by the near field length.

$$S_F = Z_F / N = Z_F (\lambda / r^2) \tag{24}$$

For point target or small ball reflectors, $S_F \leq 1$.[14]

For flat plate reflectors, $S_F \leq 1.18$.[15]

Point Target Focus: The focal length of a transducer assembly has been defined as the distance from the radiating surface to the point of maximum on-axis pulse/echo response. All transducers, whether focused or unfocused, produce such a maximum. (In the case of unfocused transducers, that maximum occurs at N.) Restricting consideration to the case of a circular transducer, Figure 6 shows the relationship between the radius of a spherically contoured transducer element and the normalized focal length S_F. For a

spherically contoured transducer element, R_{EFF} equals the radius of curvature. In the more common case of transducers with a refracting epoxy lens, R_{EFF} is calculated as follows:

$$R_{EFF} = R_L \; / \; 1 - n \qquad\qquad (25)$$

Where R_L is the actual lens radius and n is the refractive index $c_2 \, / \, c_1$ where c_2 is the velocity of sound in water and c_1 is the velocity of sound in the lens.[16]
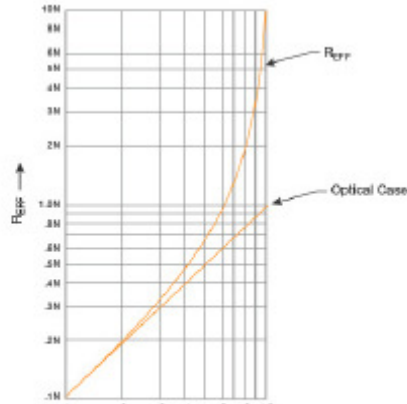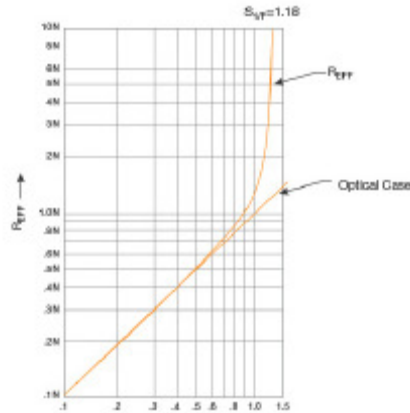

Figure 7 – Lens radius of spherically radiused circular transducer versus equivalent normalized focal length

In figure 7 the radius R_{EFF} is plotted in units of near field distance N. The straight line labeled "optical case" simply shows the relationship that should exist if the behavior of acoustic lenses was controlled by optical laws rather than diffraction. The curve labeled R_{EFF} is the actual relationship. This curve is calculated from the expression published by Wustenberg [17]

$$R_{EFF} \approx N \left(\frac{1}{1-S_F} \right) (S_F - 0.82 \, S_F^2 + 0.43 \, S_F^3) \qquad\qquad (26)$$

This curves shows, for example, that in order to produce a focus as measured by the maximum amplitude echo from a small ball target at $S_F = 0.6$, the R_{EFF} would have to be equal to N. As R_{EFF} approaches infinity, the normalized focal length approaches 1.

Flat Plate Focus: Although the true pulse/echo focal length is best measured using a ball target, the flat plate maximum response is often easier to measure, and has significance in applications where plane boundaries are measured as in many thickness gaging applications. Further, the flat plate focus us approximately related to the ball target focus.

Figure 8 -- Lens radius of spherically radiused circular transducer versus equivalent flat plate normalized focal length

Figure 8 relates the effective radius of curvature to the normalized flat plate focus. The flat plate focus is defined as the distance at which the maximum echo amplitude is observed. The flat plate focus approaches $S_F = 1.18$ as R_{EFF} approaches infinity (flat transducer), and as the flat plate focus approaches this limit the peak becomes very broad and very weak. The increase in signal amplitude at the peak is only about 0.3 dB for a flat transducer[5]. Therefore, for higher frequency transducers with large values of N, the peak in the flat plate echo amplitude may not be observed, especially if measured in water due to the offsetting effect of attenuation with increasing distance.

It is useful to have a relationship between the point target focus and the flat plate focus of a focused transducer. Figure 9 should an experimentally obtained curve of the ratio of point target focus to flat plate focus versus the effective radius of curvature. At very sharp focuses ($R_{EFF} \leq 0.1$ N) there is practically no difference between the point target focus and the flat plate focus. As the focus becomes weaker, the ratio of point target focus to flat plate focus decreases to a minimum value of about 0.66 at $R_{EFF} = 1.2$ N. The ratio begins to increase again, approaching a value of 0.85 as R_{EFF} approaches infinity. The importance of this curve is that it allows conversion of point target focal length to flat plate focal length and vice versa for any focused transducer assembly.
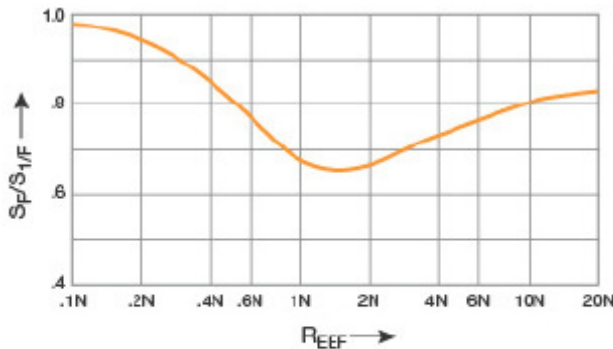
Figure 9 – Ratio of true focus to flat plate versus radius of equivalent spherically radiused circular transducer

Focal Zone: The focal zone of a focused transducer is defined as the distance between the on-axis points at which the pulse/echo signal amplitude drops to 50% (-6 dB) of the maximum amplitude at the focal point. The focal zone FZ, as drawn in Figure 10, is given by Wustenberg[17] as

$$FZ = N \left(S_F^2\right) \left[\frac{2}{1+0.5\,S_F}\right] \tag{27}$$
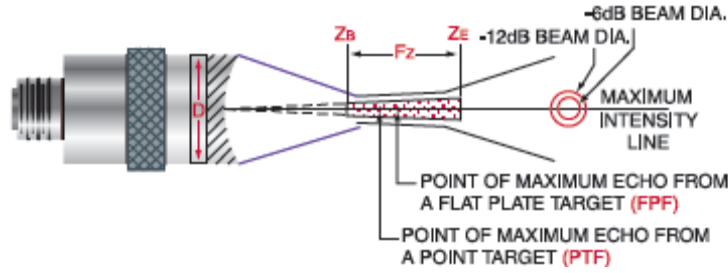
Figure 10 – Axial and transverse parameters of a focused sound beam

Wustenberg also gives the length of the part of the focal zone ΔFZ located on the near side of the focal point as

$$\Delta FZ = \frac{FZ}{4} \left[\, 1 + (1 - S_F)^2 \,\right] \tag{28}$$

It is possible to normalize the focal zone as well as the -6 dB beginning and ending points of the focal zone (S_B and S_E of Figure 9) in terms of N:

$$\frac{FZ}{N} = S_F^2 \left[\frac{2}{1-0.5S_F}\right] \tag{29}$$

$$\frac{\Delta FZ}{N} = \frac{FZ/N}{4} \left[\, 1 + (1 - S_F)^2 \,\right] \tag{30}$$

$$S_B = S_F - \frac{\Delta FZ}{N} \tag{31}$$

$$S_E = S_F + \frac{FZ}{N} - \frac{\Delta FZ}{N} = S_B + \frac{FZ}{N} \tag{32}$$

Figure 11 shows the relationship between the -6 dB focal zone expressed in terms of N, the near field length, and the normalized focal length as calculated from Wustenberg's equations. Figure 10 shows that the beginning of the focal zone is always closer to the focal point than the ending point. Both Figures 11 and 12 predict results that would be

obtained by measuring the echo amplitude from a small ball reflector using long RF excitation pulses.
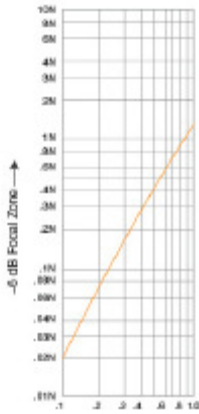
Figure 11 – Focal zone of focused Transducer assemblies versus normalized focal length
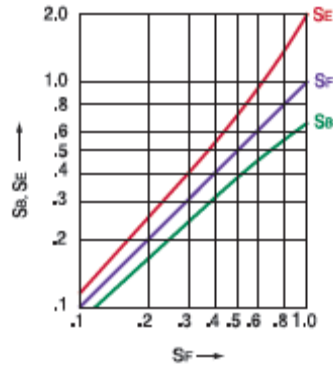
Figure 12 – Normalized beginning and ending points of the -6dB focal Zone as measured by amplitude of signal from small ball target

Effect of Focusing on Sensitivity: One of the major reasons for using focused transducer assemblies is to achieve increased pulse/echo signal amplitude from small on-axis targets such as cracks, voids, or inclusions. Kossoff[18] provides an expression for the on-axis sound intensity as a function of distance from the transducer. Relative differences in radiated sound intensity are equivalent to relative differences in echo amplitude.

$$I = \left(K \ \sin \frac{\pi N}{2KZ} \right)^2 \tag{33}$$

As Z approaches R_{EFF}, equation 33 reduces to

$$I = \left(\frac{\pi N}{2R_{EFF}} \right)^2 \tag{34}$$

Kossoff's equation has been evaluated to determine the relative maximum on-axis echo amplitude and the points at which the on-axis echo amplitude drops -6 dB from that maximum. Figure 13 shows the increase in echo amplitude that can be expected from small on-axis targets at the acoustic focus as a function of the normalized focal length S_F. Relative to an unfocused transducer, an increase in echo amplitude of 100x or 40 dB is achievable with an S_F of 0.15. However, as seen from Figure 11, under that condition the focal zone is very short, so the gain in amplitude is achieved only over a relatively small range. The -6 dB focal zone obtained from Kossoff's equation agrees very well with Wustenberg's calculation, as shown in Figure 12.
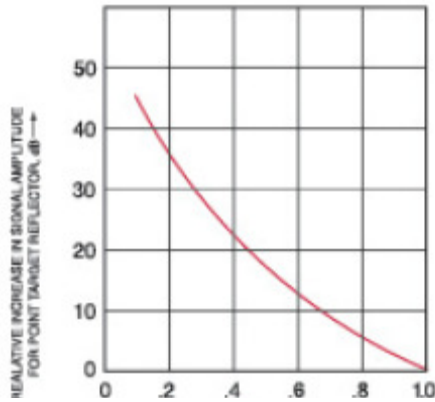
Figure 13 – Increase in on-axis pulse/echo sensitivity versus normalized focal length

Degree of Focusing: Literature often describes focusing as strong, medium or weak, but frequently there is no further definition as to what these terms mean. Schengermann[13] has proposed that degree of focusing be classified as follows:

Weak focusing $.66 < S_F \leq 1$
Medium focusing $.33 < S_F \leq .66$
Strong focusing $0 < S_F \leq .33$

Kossoff[18] suggests the following:

Weak focusing $.4 < S_F \leq 1$
Medium focusing $.15 < S_F \leq .4$
Strong focusing $0 < S_F \leq .15$

Kossoff's classifications are based on the increase in on-axis sound intensity achieved relative to a flat transducer. For weak focusing, a gain in sound intensity or echo amplitude of 10x can be realized at $S_F = 0.4$, while the gain is 100x at $S_F = 0.15$. Notwithstanding the logic of Kossoff's proposal, Schlengermann's classifications better fit actual practice. It is quite rare for transducers designed for ultrasonic NDT applications to have normalized focal lengths S_F less than 0.15.

Beam Width: Beam width is defined as the transverse distance between two points at a specified distance from the transducer where the pulse/echo signal amplitude from a small ball target reflector drops by a specified amount from the maximum on-axis amplitude. Usually the beam width is specified at the -6 dB or half peak amplitude level of a pulse/echo signal. This is equal to a -3 dB or .707 drop in transmitted pressure as it would be measured with a small hydrophone.

Beam width at the focus of a circular disk transducer can be calculated from the normalized focal length and the diameter of the transducer, or alternately from the focal length, wavelength in the test material, and element diameter:

$$BW_{-6\,dB} = 0.2568D\,S_F = 1.028\,\frac{Z_F\lambda}{D} \tag{35}$$

$$BW_{-20\,dB} = 0.435D\,S_F = 1.74\,\frac{Z_F\lambda}{D} \tag{36}$$

where D = element diameter and Z_F = focal length. The pulse/echo beam widths as defined above are calculated from the beam angle equations found in the Beam Spreading section.

Kossoff gives an equation that described a beam width that he finds closely corresponds to that measured for moderately damped transducers at – 20 dB echo amplitude relative to the on-axis peak as a function of distance:

$$BW_{-20\,dB} = \frac{0.96\,D}{K\,\sin\dfrac{\pi N}{2KZ}} \tag{37}$$

Kossoff finds this relationship to hold over the range of Z where the axial intensity or on-axis echo amplitude at least 20% of its value at the focus. It will be noted that at the acoustic focus the -20 dB width as predicted by Kossoff's equation is much larger than calculated for single frequency operation. The correspondence between equation 37 and experimental results using moderately broadbanded transducers is probably due to the effects of bandwidth.

The -6 dB beam width is often used for comparison of performance. Restated for -6 dB, Kossoff's equation becomes:

$$BW_{-6\,dB} = \frac{0.403\,D}{K\,\sin\dfrac{\pi N}{2KZ}} \tag{38}$$

This is strictly valid only for CW or long pulse operation, but comparison of the results of equation 38 with experimental measurements are in relatively good agreement for transducers with bandwidths of up to 60%. Experimentally, it has been noted that at distances within the near -6 dB range (axially) from the focus, the beam width is smaller than predicted by equation 38, falling between the beam width at the focus and the beamwidth predicted by the equation. For transducers with greater bandwith, these equations based on single frequency CW excitation become progressively less exact.

Focal Length Variation Due to Acoustic Velocity of Test Material: The measured focal length of a transducer is dependent on the medium in which it is being measured, due to the fact that different materials have different sound velocities. Transducer focal lengths are typically specified for water. Since most test materials have a higher sound velocity than water, the focal length is effectively shortened. This effect is caused by refraction and is illustrated in Figure 14.
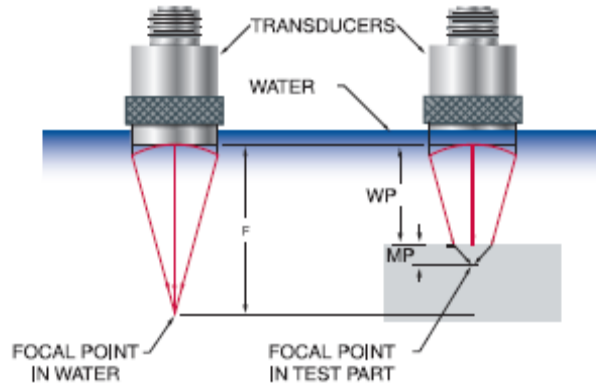
Figure 14 – Focal length variation due to material velocity

This change in focal length can be calculated with equation 39. Given a particular focal length and material path, it can be used to determine the appropriate water path with respect to the shortened focus in the test material.

$$WP = F - MP \ (c_{tm} / c_w) \tag{39}$$

where WP = one-way water path length
          MP = one-way sound path to focus in material
          F = focal length in water
          c_{tm} = sound velocity in the test material
          c_w = sound velocity in water

IV. Attenuation Effects

Attenuation is a function of frequency. The measured focal characteristics of broadband transducer assemblies with a high center frequency and/or long focal length may deviate from the expected performance due to the effect of frequency dependent attenuation in water, which effectively shifts the transducer's frequency spectrum downward by more strongly attenuating its higher frequency components. This frequency downshift also shortens the measured focal length of focused high frequency immersion transducers. Attenuation is observed as the decrease in measured signal amplitude with increasing propagation in the sound transmitting medium. Neglecting other losses such as beam spreading and diffraction, attenuation can be expressed as an exponential equation of the form:

$$A = A_0 \ e^{-\alpha f^n Z} \tag{39}$$

where Z = propagation distance in cm
       f = frequency in Hertz
       n = exponent of frequency dependence

α = frequency dependent amplitude attenuation coefficient of the medium in Nepers/cm/Hz^n

A_0 = unattenuated amplitude

A = attenuated amplitude

Attenuation in terms of dB/cm at a specific frequency is obtained from

$$dB/cm = -8.6859\ \alpha f^n$$

For water, the exponent of frequency dependence is $n = 2$.

The frequency dependence of attenuation has important consequences for the spectrum of a propagating wave. The higher frequencies are disproportionately attenuated, causing the spectrum peak frequency to shift downward with increasing propagation distance. An approximately expression for the downshifted peak frequency where the exponent of frequency dependence is 2 as in water, is given by Ophir and Jaeger[19].

$$F_{peak} = \frac{f_0}{2\alpha Z \sigma^2 + 1} \tag{40}$$

where
f_0 = unattenuated peak frequency
α = amplitude attenuation coefficient Nepers/cm/Hz^2
Z = propagation distance in cm
σ = $(f_0)(\%BW)/236$
$\%BW$ = percent bandwidth (-6 dB) of the unattenuated spectrum

This effect is quite significant at higher frequencies and longer water paths. An equation that calculates the round trip water path length that causes a 5% peak frequency downshift in water is:

$$Z = \frac{1465.68}{\alpha\ F_0^{\ 2}\ (\%BW)^2} \tag{41}$$

Table 1 that follows has been calculated in this manner. It shows the total (round trip) water path length that would be expected to produce a 5% downshift in peak frequency for transducers of various bandwidths and unattenuated peak frequencies.

Table 1 – Guideline for Total Maximum Water Path (millimeters)

Maximum total water path, with respect to frequency and bandwidth, producing frequency downshift no greater than 5%. Note that for pulse/echo testing, these numbers must be divided by two to obtain the distance between the transducer and the test piece.

MHz	BW 30%	40%	50%	60%	70%	80%	90%	100%
2.25	--	--	--	--	--	--	--	--
3.5	--	--	--	--	660	510	405	330
5.0	--	--	635	430	330	255	175	150
7.5	--	430	280	175	125	100	75	50
10.0	430	255	150	100	75	50	25	25
15.0	175	100	50	25	25	25	29	18
20.0	100	50	25	25	20	15	10	10
25.0	50	25	25	18	12	10	7.5	5
30.0	25	25	18	10	7.5	5	5	2.5
40.0	25	15	10	5	5	2.5	2.5	2.5
50.0	18	10	5	2.5	2.5	2.5	1.8	1.5

The notation "- -" indicates a water path greater than 750 mm.

This table uses an attenuation coefficient α for water of -3.12 times 10^{-3} db/cm/MHz^2. Notice that as bandwidth increases at a given frequency, the permissible water path decreases. If the combination of center frequency, bandwidth, and water path as determined by focal length and test requirements are beyond the limits indicated in Table 1, it may be possible to use a shorter focal length to permit a shorter water path. At the same time, it is clear that water path attenuation effects significantly limit water path length at higher test frequencies.

References

(1) J. L Rose, *Materials Evaluation*, pp. 114-120, May 1976

(2) H. Wustenberg, E. Schultz, IIW Document VC-345-78/OE

(3) R. S. Gilmore, G. J. Czerw, "Ultrasonic Spectroscopy for Flaw Characterization", General Electric Technical Information Series 75MPL 404, January 8, 1976

(4) H. Seki, A. Ganto, H. Truell, *J. Acoust. Soc. Amer*. 28, pp. 230-238 (1954)

(5) E. P. Papadakis, *J. Acoust. Soc. Amer*. 40, pp. 863-876 (1966)

(6) R. C. McMasters, *Nondestructive Testing Handbook* (Ronald Press, New York, 1959, Volume II, Sec. 44, pp. 12-19

(7) J. Zemanek, *J. Acoust. Soc. Amer.* 49, pp. 181-191 (1971)

(8) J. W. Goodman*, Introduction to Fourier Optics*, McGraw Hill, 1968

(9) G. J. Posakony, IEEE Ultrasonics Symposium Proceedings, pp. 1-9, 1975. IEEE Cat. #75 CHO994-450

(10) E. P. Papadakis, and K. A. Fowler, *J. Acoust. Soc. Amer.* 50, pp. 729-745 (1971)

(11) G. P. Single and J. L. Rose, *Mat. Eval.*, Vol. 40, pp. 880-885, July 1982

(12) W. L. Beaver, *J. Acoust. Soc. Amer.* 56, No. 4, pp. 1043-1048 (October 1974)

(13) U. Schlengermann, *Mat. Eval.*, Vol. 40, pp. 73-89, December 1980

(14) U. Schlengermann, NASA TM 75309

(15) E. P. Papadakis, *J. Acoust. Soc. Amer.* 40, pp. 863-876 (October 1966)

(16) E. P. Papadakis, *International Journal of NDT*, Vol. 4, pp. 195-198 (1972)

(17) H. Wustenberg, E. Schenk, and W. Mohrle, *I. Mech. E.* 1982

(18) G. Kossoff, Ultrasound in Med. And Biol., Vol. 5, pp. 359-365, Pergamon Press Ltd. (1979)

(19) J. Ophir and P. Jaeger, *Ultrasonic Imaging*, Vol. 4, pp. 282-289 (1982)